Iron(III) Complexes as Superoxide Dismutase Mimics: Synthesis, Characterization, Crystal Structure, and Superoxide Dismutase (SOD) Activity of Iron(III) Complexes Containing Pentaaza Macrocyclic Ligands

DeLong Zhang,[†] Daryle H. Busch,*[,†] Patrick L. Lennon,[‡] Randy H. Weiss,[‡] William L. Neumann,[‡] and Dennis P. Riley*[,‡]

Chemistry Department, The University of Kansas, Malott Hall, Lawrence, Kansas 66045, and Monsanto Corporate Research Division, Monsanto Company, 800 North Lindbergh Boulevard, St. Louis, Missouri 63167

Received July 9, 1997

Iron(III) complexes with four pentaaza macrocyclic ligands, $[Fe(L)Cl_2](PF_6)$, have been synthesized, where the ligand L is 1,4,7,10,13-pentaazacyclopentadecane (L^1), 2*R*,3*R*,8*S*,9*S*-dicyclohexano-1,4,7,10,13-pentaazacyclopentadecane (L^2), 2*R*,3*R*,8*R*,9*R* -dicyclohexano-1,4,7,10,13-pentaazacyclopentadecane (L^3), or 2*S*,*5R*,*8S*,*11R*,*14S*-pentamethyl-1,4,7,10,13-pentaazacyclopentadecane (L^4), respectively. Conductivity measurements in acetonitrile are consistent with two chloro anions coordinated to iron(III). In acetonitrile solution, all four iron complexes exhibit a reversible or quasi-reversible redox couple in the experimental range −1.5 to +1.5 V vs E_{Ag/Ag^+}, and the redox potentials for those four complexes are similar (from −0.15 to −0.19 V vs NHE). In aqueous solutions, the electrochemical properties of those complexes are different from those in acetonitrile solution; the redox peaks shift more than 0.5 V more positive. The complexes with L^1, L^2, and L^3 display a reversible redox at 0.35, 0.45, and 0.43 V vs NHE, respectively, while $[Fe(L^4)Cl_2](PF_6)$ shows a cathodic peak at 0.44 V and two anodic peaks at 0.31 and 0.14 V vs NHE, respectively. The base titration results reveal that two water molecules are coordinated to the iron(III) in these complexes. pK_{a1} and pK_{a2}: 3.46(7) and 7.31(7) for $[Fe(L^1)Cl_2](PF_6)$; 3.7(1) and 7.50(2) for $[Fe(L^2)Cl_2](PF_6)$; 4.1(1) and 7.73(2) for $[Fe(L^3)Cl_2](PF_6)$; 3.6(7) and 7.4(2) for $[Fe(L^4)Cl_2](PF_6)$. The superoxide dismutase (SOD) activity, assessed by stopped-flow experiments, reveals that all four metal complexes catalyze the fast disproportionation of superoxide in aqueous solution: at pH = 7.8, the catalyic rate constants for the complexes were 0.81×10^7, 1.42×10^7, 1.41×10^7, and 0.29×10^7 M^{-1} s^{-1} for $[Fe(L^1)Cl_2](PF_6)$, $[Fe(L^2)Cl_2](PF_6)$, $[Fe(L^3)Cl_2](PF_6)$, and $[Fe(L^4)Cl_2](PF_6)$, respectively. The crystal structure of $[Fe(L^2)Cl_2](PF_6)$ was determined. Crystal data: triclinic, $P\bar{1}$; $a = 7.367(2)$, $b = 10.707(2)$, $c = 17.632(2)$ Å; $\alpha = 81.27(2)$, $\beta = 79.74(2)$, $\gamma = 83.38(2)°$; $R = 0.0465$ for observed data ($I > 2\sigma(I)$). The iron is seven-coordinate with five nitrogen atoms from the pentaaza macrocylic ligand and *trans*-chloro anions in a pentagonal bipyramidal arrangement. The average bond lengths for Fe−N and Fe−Cl are 2.271 and 2.339 Å, respectively.

Introduction

A considerable amount of experimental data suggests that inflamed tissue and tissue subjected to ischemia followed by reperfusion are under severe oxidative stress induced by the one-electron-reduction product of oxygen, superoxide, produced by the NADPH oxidase-mediated univalent reduction of molecular oxygen.[1−5] Superoxide dismutase (SOD), which can destroy the superoxide very rapidly, is Nature's agent for protection of the organism from this radical burden. In fact, native SOD enzymes have been shown in many studies to exhibit protection in animal models of inflammatory diseases.[6] In a variety of scenarios, therapeutic dosage of additional SOD enzyme has shown promise, but from a number of viewpoints (stability, tissue permeability, oral bioavailability, specific tissue targeting, immunogenicity, etc.) synthetic metal complexes offer considerable promise as SOD catalysts for pharmaceutical applications.

Depending on the metal at the active center, there are three general types of SOD enzymes, namely Cu/Zn−SOD and Mn−SOD in mammalian systems and Fe−SOD in bacterial systems. Largely due to toxicity issues, we have focused our efforts on the design of Mn(II)-based complexes as SOD mimics and have achieved remarkable success in generating highly stable Mn(II) complexes with outstanding catalytic SOD activity.[7,8] The ligands utilized in these synthetic Mn(II)-based mimics are of the same class as we report here; namely, the 1,4,7,10,13-pentaazacyclopentadecane (L^1) type ligand and its C-substituted derivatives. Since iron is a most relevant metal for the design of synthetic SOD catalysts, we also embarked on an effort to discover macrocyclic Fe complexes capable of dismuting superoxide at bimolecular rates in excess of $1 \times 10^{+6}$ M^{-1} s^{-1} (for comparison the Mn(II) complexes of the [15]aneN_5 ligands exhibit rates generally in excess of 10^{+7} M^{-1} s^{-1}).[7,8] While a

* To whom correspondence should be addressed.
[†] The University of Kansas.
[‡] Monsanto Co.

(1) McCord, J. M. *New Horizons* **1993**, *1*, 70.
(2) Kilgore, K. S.; Lucchesi, B. R. *Clin. Biochem.* **1993**, *26*, 359.
(3) Halliwell, B. *Lancet* **1994**, *344*, 721.
(4) Grisham, M. B. *Lancet* **1994**, *344*, 859.
(5) Chen, L. Y.; Nichols, W. W.; Hendricks, J.; Mehta, J. L. *Am. Heart J.* **1995**, *129*, 211.
(6) McCord, J. M. *Free Radicals Biol. Med.* **1986**, *2*, 307.
(7) Riley, D. P.; Weiss, R. H. *J. Am. Chem. Soc.* **1994**, *116*, 387.
(8) Riley, D. P.; Henke, S. L.; Lennon, P. L.; Weiss, R. H.; Neumann, W. L.; Rivers, W. J.; Aston, K. W.; Sample, K. R.; Rahman, H.; Ling, C.-S.; Shieh, J.-J.; Busch, D. H.; Szulbinski, W. *Inorg. Chem.* **1996**, *35*, 5213.

S0020-1669(97)00861-6 CCC: $15.00
Published on Web 02/04/1998

few Fe^{II} and Fe^{III} complexes have been reported to behave as SOD mimics, their SOD activity was not directly measured.[9−12] Herein we report the synthesis, characterization, and SOD activity of four new Fe^{III} complexes with [15]aneN_5 type ligands. The SOD activities of these complexes have been measured by the stopped-flow technique[13] and are also reported here.

Experimental Section

Synthesis. L^1 was synthesized as reported in ref 7, L^2 was synthesized as reported in ref 8, and ligands L^3 and L^4 were synthesized according to the methods of ref 14 .

(a) [Fe(L^1)Cl](PF$_6$). In a glovebox, ligand L^1 (0.50 mmol) was dissolved in 0.5 mL of methanol, and 2 mL of an $FeCl_2$ (0.50 mmol)−methanol solution was slowly added under stirring. The mixture was stirred for 2 h before it was filtered to remove any insolubles. To the filtrate was added a clear solution of ammonium hexafluorophosphate (1 mmol). The resulting solution was slowly cooled to room temperature and allowed to stand overnight. The off-white solid was collected by filtration and washed with 2 mL of methanol. Yield: 0.185 g (0.41 mmol) or 82%. Anal. Calc for $C_{10}H_{20}N_5ClFeF_6P(CH_3OH)$: H, 6.04; C, 27.32; N, 14.48. Found: H, 6.00; C, 27.18; N, 14.70.

(b) [Fe(L^1)Cl$_2$](PF$_6$). In a glovebox, $FeCl_3$ (0.5 mmol) was dissolved in 2 mL of pyridine. This solution was added to 0.5 mmol of ligand in methanol under stirring, and the resulting solution was heated for 2 h. After the solution was cooled to room temperature and filtered, a clear solution of ammonium hexafluorophosphate was added to obtain a yellow precipitate. Yield: 0.170 g (0.338 mmol) or 68%. Anal. Calc for $C_{10}H_{20}N_5FeF_6P(CH_3OH)_{0.5}$: H, 5.41; C, 25.07; N, 13.92. Found: H, 5.60; C, 25.18; N, 13.89. The product was recrystallized from acetonitrile solution. Anal. Calc for $C_{10}H_{20}N_5Cl_2FeF_6P$: H, 4.18; C, 24.92; N, 14.53. Found: H, 4.99; C, 25.00; N, 14.60. In the mass spectrum, two peaks at $m/e = 306$ and 341 were observed and assigned to $([Fe(L^1)Cl]^{2+} + e)^+$ and $[Fe(L^1)Cl_2]^+$, respectively.

(c) [Fe(L^2)Cl$_2$](PF$_6$). In a glovebox, 0.3 mmol of L^2 was dissolved in 1 mL of methanol, and 0.3 mmol of $FeCl_3$ in pyridine (1.5 mL) was added to the ligand under stirring. After 3 h of heating, the solution was filtered. To the filtrate was added a clear solution containing 0.1 g (0.6 mmol) of NH_4PF_6. The mixture was evaporated to dryness. Methanol (2 mL) was added to the residue, and the mixture was stirred for 2 h. The greenish yellow solid was collected via filtration and washed with methanol. Yield: 0.10 g or 56%. Anal. Calc for $C_{18}H_{37}N_5Cl_2FeF_6P$: H, 6.28; C, 36.35; N, 11.78. Found: H, 6.22; C, 36.16; N, 11.59. The product was recrystallized from a mixture of acetonitrile and ethanol to obtain crystals of X-ray quality.

(d) [Fe(L^3)Cl$_2$](PF$_6$). In a glovebox, 0.3 mmol of $FeCl_3$ was added to 1 mL of pyridine, and 0.3 mmol of L^3 in methanol (1 mL) was added. The mixture was heated and stirred for 3 h to obtain a brownish solution, which was filtered after cooling to room temperature. To the filtrate was added a clear solution containing 0.12 g (0.7 mmol) of NH_4PF_6. The mixture was evaporated to dryness. Acetonitrile (2 mL) was added to the residue, and the mixture was stirred for 2 h before it was filtered. The filtrate was evaporated to obtain a solid, which was then dissolved in methanol. Upon slow evaporation, a greenish yellow solid formed and was collected by filtration. The product was dissolved in ethanol, and another greenish solid was obtained upon evaporation of the solvent. The solid was filtered off and dried. Yield: 75 mg or 42%. Anal. Calc for $C_{18}H_{37}N_5Cl_2FeF_6P$: H, 6.28; C, 36.35; N, 11.78. Found: H, 6.10; C, 36.22; N, 11.58.

(e) [Fe(L^4)Cl$_2$](PF$_6$). The crude product of this complex was prepared by using a procedure similar to that for [Fe(L^3)Cl$_2$](PF$_6$). Crystals were obtained by recrystallization of the crude product from a mixture of acetonitrile and ethanol. Anal. Calc for $C_{15}H_{35}N_5Cl_2F_6FeP$: H, 6.34; C, 32.37; N, 12.59. Found: H, 6.30; C, 32.44; N, 12.40.

Instrumentation. Electrochemical experiments were performed on a Princeton Applied Research model 175 programmer and model 173 potentiostat. The output was recorded using a Houston Instruments recorder. A glassy carbon electrode, a silver wire, and a platinum wire were used as working, reference, and secondary electrodes, respectively. Under nitrogen, acetonitrile solutions of the complexes (1−2 mM) with tetrabutylammonium tetrafluoroborate(0.1 M) as a supporting electrolyte were used in the experiments. The potentials vs NHE were determined by using ferrocene as internal reference in organic solvents, typically acetonitrile, and adding 0.41 V to the observed voltages vs $E_{Fc/Fc+}$. In aqueous solution, a saturated calomel electrode was used as the reference electrode, and the potential vs NHE was calibrated by the SCE potential (0.24 vs NHE).

A YSI model 35 conductance meter was used to measure the molar conductivity. Usually 5 mL of an acetonitrile solution of the complex was prepared in a 25 mL test tube, and the typical concentration for the solutions was around 1×10^{-3} M.

The proton dissociation constants of the water molecules coordinated to metal centers were determined by a potentiometric method. Typically, about 3 mg of sample was dissolved in 2 mL of boiled deionized water under nitrogen, and a NaOH solution (1.010 M) in a 10 μL syringe was used to titrate the complex solution, while the pH was measured by an Accumet pH meter, model 805 MP, from Fisher Scientific. The titration was carried out under a nitrogen atmosphere. The pH of the solution was recorded after every addition of 0.2 μL of NaOH solution, and the data were processed by the PKAS program.[15]

The rate constant for the catalyzed superoxide dismutation reaction of superoxide was measured by the stopped-flow spectrophotometric methods reported previously[13] and by utilizing an OLIS rapid-scan spectrophotometer/stopped-flow system. In general, the Fe^{III}(L) complexes were dissolved in 80 mM HEPES buffer solutions, and the saturated KO_2 solution (∼0.2 M) in DMSO was freshly prepared. On the instrument, an aqueous solution of the complex and DMSO solution of KO_2 (mixing ratio: 19/1 water to DMSO) were injected into the mixing cell from two syringes, and the decay of absorbance of superoxide ($\lambda_{max} = 245$ nm) was monitored. The background decay of superoxide itself is second-order and at the pH range utilized in these studies (7.4−8.1) is much slower than the catalytic rates measured with these catalysts when they are utilized at the 10^{-6} M concentration range.[13] Additionally, the control reactions of free ligand and $FeCl_3$ in buffer at pH = 7.4 show no catalytic activity (the ferric chloride solutions age rapidly generating olated insoluble products). The data were exported as text files which were processed in the graphic program Cricket Graph. The variation of the absorbance with time provided the observed rate constant k_{obs}.

X-ray Crystal Structure. A single crystal of **[Fe(L^2)Cl$_2$](PF$_6$)** of $0.6 \times 0.3 \times 0.1$ mm dimensions was mounted on a glass fiber in random orientation. Data collection was performed on a Siemens P4RA automated single-crystal X-ray diffractometer using graphite-monochromated Mo Kα radiation ($\lambda = 0.710\ 73$ Å) at 25 °C. Autoindexing of 15 centered reflections from the rotation photograph indicated a triclinic lattice. Equivalent reflections were checked to confirm the Laue symmetry, and fractional index search was conducted to confirm the cell lengths (XSCANS, Siemens Analytical Instruments, Madison, WI, 1994). Final cell constants and orientation matrix for data collection were calculated by least-squares refinement of the setting angles for 36 reflections ($9° < \theta < 25°$). Intensity data were collected using $\bar{\omega}-2\theta$ scans with variable scan speed. Three representative reflections measured every 97 reflections showed 17.6% variation during data collection. Crystal data and intensity data collection parameters are listed in Table 3.

Data reduction was carried out using XSCANS, and structure solution and refinement were carried out using the SHELXTL-Plus (5.03)

(9) Bull, C.; McClune, G. J.; Fee, J. A. *J. Am. Chem. Soc.* **1983**, *105*, 5290.
(10) Nagano, T.; Hirano, T.; Hirobe, M. *J. Biol. Chem.* **1989**, *264*, 9243.
(11) Nagano, T.; Hirano, T.; Hirobe, M. *Free Radical Res. Commun.* **1991**, *12*, 221.
(12) Iuliano, L.; Pedersen, J. Z.; Ghiselli, A.; Pratico, D.; Rotilio, G.; Violi, F. *Arch. Biochem. Biophys.* **1992**, *293*, 153.
(13) Riley, D. P.; Rivers, W. J.; Weiss, R. H. *Anal. Biochem.* **1991**, *196*, 344.
(14) Lennon, P. J.; Rahman, H.; Aston, K. W.; Henke, S. L.; Riley, D. P. *Tetrahedron Lett.* **1994**, *35*, 853.
(15) Martell, A. E.; Motekaitis, R. J. *Determination and Use of Stability Constants*; VCH Publishers, Inc.: New York, 1988; p 159.

Table 1. Proton Dissociation Constants for the Aqua Ligands of the Fe^{III} Complexes

complex	pK_{a1}	pK_{a2}	complex	pK_{a1}	pK_{a2}
$[FeL^1Cl_2](PF_6)$	3.46(7)	7.31(7)	$[FeL^3Cl_2](PF_6)$	4.1(1)	7.73(2)
$[FeL^2Cl_2](PF_6)$	3.7(1)	7.50(5)	$[FeL^4Cl_2](PF_6)$	3.6(3)	7.4(2)

Table 2. Redox Potentials for the Fe^{III} Complexes in Acetonitrile and Aqueous Solution with the Peak Separation (mV) in Parentheses

	$E_{1/2}$ (V vs NHE)	
complex	CH_3CN	H_2O
$[FeL^1Cl_2](PF_6)$	−0.17 (75)	0.35 (75)
$[FeL^2Cl_2](PF_6)$	−0.15 (80)	0.45 (80)
$[FeL^3Cl_2](PF_6)$	−0.18 (90)	0.43 (80)
$[FeL^4Cl_2](PF_6)$	−0.19 (75)	0.44 (E_{ap}),[a] 0.31 (E_{cp}), 0.14 (E_{cp})

[a] E_{ap} and E_{cp} are the potentials for anodic and cathodic peaks, respectively.

Table 3. Crystal Data and Structure Refinement Parameters for $[Fe(L^2)Cl_2](PF_6)$

empirical formula: $C_{18.50}H_{39}Cl_2F_6FeN_5O_{0.5}P$
formula weight: 611.27
temperature: 293(2) K
wavelength: 0.710 73 Å
crystal system: triclinic
space group: $P\bar{1}$
unit cell dimensions: $a = 7.3671(5)$ Å, $b = 10.7063(7)$ Å, $c = 17.631(2)$ Å
$\alpha = 81.269(8)°$ $\beta = 79.736(8)°$, $\gamma = 83.388(7)°$
volume, Z: 1347.0(2) Å^3, 2
density (calcd):1.507 g/cm^3
absorption coefficient: 0.878 mm^{-1}
$F(000)$: 636
crystal size: 0.6 × 0.3 × 0.1 mm
θ range for data collection: 1.93−28.00°
limiting indices: $-1 \le h \le 10$, $-14 \le k \le 14$, $-24 \le l \le 24$
no. of reflections collected: 7989
no. of independent reflections: 6498 ($R_{int} = 0.0239$)
absorption correction: semiempirical from ψ-scans
max and min transmission: 0.8802 and 0.7396
refinement method: full-matrix least-squares on F^2
data/restraints/parameters: 6426/1/339
goodness-of-fit on F^2: 1.029
final R indices [$I > 2\sigma(I)$]: R1 = 0.0465, wR2 = 0.1161
R indices (all data): R1 = 0.0782, wR2 = 0.1366
largest diff peak and hole: 0.544 and −0.341 e Å^{-3}

software package (G. M. Sheldrick, Siemens Analytical Instruments, Madison, WI, 1995). Linear decay correction was applied to the data, and absorption correction was carried out using Ψ-scan and equivalent reflections. The structure was solved by direct methods and refined successfully in the triclinic space group $P\bar{1}$. Full-matrix least-squares refinement was carried out by minimizing $\sum w(F_o^2 - F_c^2)^2$. The non-hydrogen atoms were refined anisotropically to convergence. The hydrogen atoms bonded to the N atoms were refined freely with isotropic thermal parameters. The rest of the hydrogens were refined using appropriate riding models. The final residual values were $R(F) = 4.65\%$ for 4424 observed reflections [$I > 2\sigma(I)$] and $R_w(F^2) = 13.7\%$; $\sigma = 1.03$ for all the data. Structure refinement parameters are listed in Table 3. The atomic coordinates ($\times 10^4$) and equivalent isotropic displacement parameters (Å^2 × 10^3) are listed in Table 6. The compound crystallizes with half a molecule of methanol per molecule of complex. The solvent molecule is disordered. The occupancy factor could not be refined as the solvent molecule is located near the center of inversion and occupies one of the two symmetry-related sites 50% of the time.

Results and Discussion

Synthesis and Characterization. Since the pentaazacycloalkane ligand has five saturated secondary amine N donors, the iron complexes are expected to exhibit very low $Fe^{II/III}$ redox potentials, resulting in Fe^{II} complexes which are readily oxidized and should be very unstable in air. Accordingly, we observe that the off-white Fe^{II} complex with L^1 quickly turns brown after exposure to air. Consequently, for reasons of stability and ease of handling, we prepared the Fe^{III} complexes of these pentaazacyclopentadecane ligands for the studies on their SOD activity.

Both Fe(II) and Fe(III) complexes were prepared in a glovebox under a nitrogen atmosphere because of oxygen sensitivity issue and because of the fact that the starting materials including ligands and $FeCl_3$ are very hygroscopic. The Fe(II) complex was prepared from the reaction between the ligand and Fe(II) in methanol solution, and the complex was precipitated with PF_6^- as the counteranion after addition of ammonium hexafluorophosphate. The complexation reaction between $FeCl_3$ and ligand was carried out in pyridine: typically, an $FeCl_3$ pyridine solution (0.5 mL) is added to a vial containing the ligand in methanol. All the complexes were prepared with PF_6^- as the counterion.

Table 4. Selected Bond Lengths (Å) for $[Fe(L^2)Cl_2](PF_6)$

Fe−N(2)	2.250(3)	Fe−N(4)	2.259(3)
Fe−N(5)	2.275(2)	Fe−N(3)	2.280(3)
Fe−N(1)	2.290(3)	Fe−Cl(2)	2.3287(8)
Fe−Cl(1)	2.3501(8)	N(1)−C(1)	1.472(4)
N(1)−C(18)	1.480(4)	N(2)−C(3)	1.465(4)
N(2)−C(2)	1.468(4)	N(3)−C(4)	1.475(4)
N(3)−C(5)	1.482(4)	N(4)−C(11)	1.474(4)
N(4)−C(10)	1.480(4)	N(5)−C(12)	1.475(4)
N(5)−C(13)	1.478(4)	C(1)−C(2)	1.513(4)
C(3)−C(4)	1.498(5)	C(5)−C(10)	1.513(4)
C(5)−C(6)	1.526(4)	C(6)−C(7)	1.520(6)
C(7)−C(8)	1.534(6)	C(8)−C(9)	1.512(6)
C(9)−C(10)	1.522(5)	C(11)−C(12)	1.506(4)
C(13)−C(18)	1.513(4)	C(13)−C(14)	1.533(4)
C(15)−C(16)	1.521(6)	C(16)−C(17)	1.520(5)
C(17)−C(18)	1.521(4)		

Table 5. Selected Bond Angles (deg) for $[Fe(L^2)Cl_2](PF_6)$

N(2)−Fe−N(4)	144.97(9)	N(2)−Fe−N(5)	144.79(9)
N(4)−Fe−N(5)	69.11(9)	N(2)−Fe−N(3)	73.72(10)
N(4)−Fe−N(3)	72.67(9)	N(5)−Fe−N(3)	141.44(10)
N(2)−Fe−N(1)	73.37(9)	N(4)−Fe−N(1)	141.44(9)
N(5)−Fe−N(1)	72.39(9)	N(3)−Fe−N(1)	145.23(9)
N(2)−Fe−Cl(2)	84.88(7)	N(4)−Fe−Cl(2)	88.26(7)
N(5)−Fe−Cl(2)	89.13(7)	N(3)−Fe−Cl(2)	94.69(7)
N(1)−Fe−Cl(2)	93.28(7)	N(2)−Fe−Cl(1)	92.38(7)
N(4)−Fe−Cl(1)	94.96(7)	N(5)−Fe−Cl(1)	92.15(7)
N(3)−Fe−Cl(1)	86.15(7)	N(1)−Fe−Cl(1)	84.29(7)
Cl(2)−Fe−Cl(1)	176.77(4)	C(1)−N(1)−C(18)	115.6(2)
C(1)−N(1)−Fe	113.2(2)	C(18)−N(1)−Fe	113.1(2)
C(3)−N(2)−C(2)	114.4(2)	C(3)−N(2)−Fe	112.1(2)
C(2)−N(2)−Fe	113.7(2)	C(4)−N(3)−C(5)	115.2(2)
C(4)−N(3)−Fe	112.5(2)	C(5)−N(3)−Fe	111.0(2)
C(11)−N(4)−C(10)	112.3(2)	C(11)−N(4)−Fe	111.7(2)
C(10)−N(4)−Fe	116.8(2)	C(12)−N(5)−C(13)	112.8(2)
C(12)−N(5)−Fe	112.6(2)	C(13)−N(5)−Fe	115.9(2)
N(1)−C(1)−C(2)	106.8(3)	N(2)−C(2)−C(1)	107.6(2)
N(2)−C(3)−C(4)	106.7(3)	N(3)−C(4)−C(3)	107.4(3)
N(3)−C(5)−C(10)	106.7(2)	N(3)−C(5)−C(6)	114.9(3)
C(10)−C(5)−C(6)	10.6(3)	C(7)−C(6)−C(5)	109.9(3)
C(6)−C(7)−C(8)	111.2(3)	C(9)−C(8)−C(7)	110.6(3)
C(8)−C(9)−C(10)	110.9(4)	N(4)−C(10)−C(5)	107.9(2)
N(4)−C(10)−C(9)	113.9(3)	C(5)−C(10)−C(9)	111.2(3)
N(4)−C(11)−C(12)	110.6(3)	N(5)−C(12)−C(11)	111.5(2)
N(5)−C(13)−C(18)	108.5(2)	N(5)−C(13)−C(14)	113.6(3)
C(18)−C(13)−C(14)	111.4(3)	C(15)−C(14)−C(13)	109.9(3)
C(16)−C(15)−C(14)	111.3(3)	C(17)−C(16)−C(15)	111.1(3)
C(16)−C(17)−C(18)	111.2(3)	N(1)−C(18)−C(13)	106.1(2)
N(1)−C(18)−C(17)	115.0(3)	C(13)−C(18)−C(17)	111.0(3)

Table 6. Atomic Coordinates ($\times 10^4$) and Equivalent Isotropic Displacement Parameters ($Å^2 \times 10^3$) for $[Fe(L^2)Cl_2](PF_6)$[a]

	x	*y*	*z*	*U*(eq)
Fe	1087(1)	3887(1)	2976(1)	35(1)
Cl(1)	−1791(1)	4860(1)	3500(1)	49(1)
Cl(2)	3992(1)	2917(1)	2524(1)	48(1)
N(1)	2271(3)	5172(2)	3656(1)	39(1)
N(2)	1455(4)	2740(2)	4126(2)	41(1)
N(3)	−416(4)	2112(2)	3063(2)	44(1)
N(4)	310(4)	3839(2)	1798(2)	41(1)
N(5)	1810(3)	5678(2)	2154(2)	39(1)
C(1)	3029(5)	4476(3)	4334(2)	48(1)
C(2)	1692(5)	3508(3)	4718(2)	48(1)
C(3)	62(5)	1828(3)	4390(2)	51(1)
C(4)	7(5)	1146(3)	3714(2)	54(1)
C(5)	−174(4)	1648(3)	2298(2)	46(1)
C(6)	−1265(5)	528(3)	2281(2)	63(1)
C(7)	−943(6)	167(4)	1464(3)	76(1)
C(8)	−1474(7)	1296(4)	874(3)	86(1)
C(9)	−418(6)	2414(4)	902(2)	68(1)
C(10)	−718(4)	2767(3)	1723(2)	48(1)
C(11)	−566(5)	5074(3)	1489(2)	54(1)
C(12)	391(5)	6145(3)	1659(2)	52(1)
C(13)	2402(4)	6695(3)	2509(2)	42(1)
C(14)	3528(5)	7640(3)	1923(2)	57(1)
C(15)	4096(6)	8645(3)	2342(3)	70(1)
C(16)	5163(6)	8040(4)	2989(2)	65(1)
C(17)	4046(5)	7093(3)	3562(2)	54(1)
C(18)	3467(4)	6090(3)	3150(2)	41(1)
P(1)	5000	0	5000	51(1)
F(1)	4624(4)	−1266(2)	5577(2)	94(1)
F(2)	3464(3)	−267(3)	4535(2)	88(1)
F(3)	6564(3)	−777(2)	4463(1)	73(1)
P(2)	5000	5000	10000	58(1)
F(4)	4699(5)	5040(4)	9142(2)	140(1)
F(5)	5995(7)	3662(4)	9945(3)	171(2)
F(6)	3077(5)	4504(5)	10287(2)	162(2)
O(1)	4188(23)	689(20)	9961(10)	261(12)
C(19)	4063(26)	955(20)	10774(8)	323(21)

[a] *U*(eq) is defined as one-third of the trace of the orthogonalized $\mathbf{U}_{ij}$ tensor.

The greenish yellow Fe^{III} complex, $[Fe(L^1)Cl_2](PF_6)$, is soluble in water and acetonitrile. The corresponding Fe(III) complexes of the two stereoisomers L^2 and L^3 have markedly different solubilities. The complex $[Fe(L^2)Cl_2](PF_6)$ was much more soluble in polar organic solvents than $[Fe(L^3)Cl_2](PF_6)$, although they have the same composition and are of the same electrolyte type, 1:1. For example, $[Fe(L^2)Cl_2](PF_6)$ is only slightly soluble in methanol while $[Fe(L^3)Cl_2](PF_6)$ is very soluble. This difference in the solubility has also been observed for the tosylated ligands. The solubility of $[Fe(L^4)Cl_2](PF_6)$ was similar to that of $[Fe(L^3)Cl_2](PF_6)$. Stability is a major design consideration for candidates for human pharmaceutical applications. Thus, the determination of the stability of these Fe(III) complexes in aqueous media is of considerable importance. The complex $[Fe(L^1)Cl_2](PF_6)$ is stable in aqueous solution for several hours at physiological pH, but some precipitate does form after several days, probably due to hydrolysis. In contrast, the Fe^{III} complexes with the other three ligands are stable in aqueous solution under physiological conditions with the aqueous solutions of the complexes with L^2, L^3, and L^4 remaining clear for several months. $[Fe(L^2)Cl_2](PF_6)$ is also stable in mildly acidic solution and only decomposes slowly in 4.6 N H_2SO_4 solution. The decomposition of the complexes is evidenced by the decrease in the absorbance for the complexes (vide infra). It was found that only about 8% of $[Fe(L^2)Cl_2](PF_6)$ decomposes in 4.6 N H_2SO_4 over a period of 10 h. This indicates that the iron(III) ion forms very stable complexes with pentaazacycloalkanes.

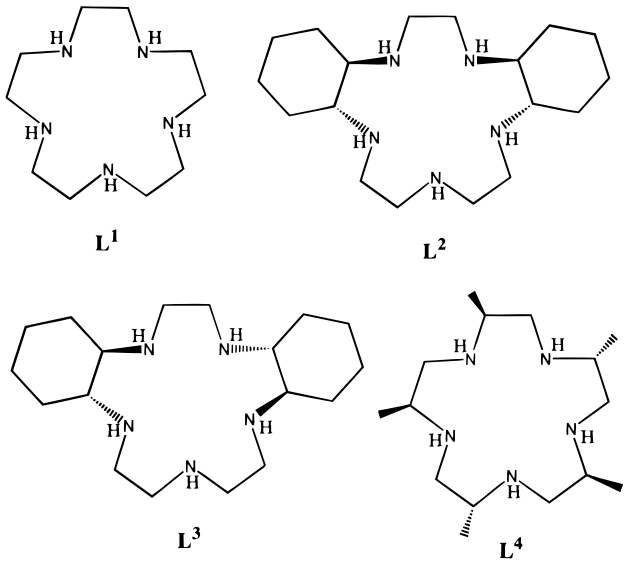

Figure 1. Structures of the pentaaza macrocyclic ligands utilized for the synthesis of Fe(III) complexes.

All four of the new Fe^{III} complexes described here were found to be high-spin d^5 complexes on the basis of the solution magnetic susceptibilities determined by NMR and Evans' method,[16] which were observed to be approximately 5.6 μ_B for the each of the four new complexes. The electronic spectrum of each new Fe^{III} complex was also recorded in HEPES buffer in water at a concentration of 1.0×10^{-4} M over a pH range of 6.0−8.1. The spectra of all the complexes were virtually identical with a λ_{max} at 294 nm (pH = 8.1) with an extinction coefficient of ∼9400 cm^{-1} M^{-1}. When the pH is lowered, the band max shifts to slightly lower energy with a lower molar extinction (λ_{max} at 306 nm ϵ ∼3100). The high-pH absorption is due to the presence of the $[Fe^{III}(L)(OH)_2]^+$ complex, and the low-pH absorption is due to the presence of the $[Fe^{III}(L)(OH)(OH_2)]^{2+}$ complex (vide infra).

Acidity of the Coordinated Water Molecules. Molar conductivity measurements in acetonitrile solution reveal that the Fe^{III} complexes $[Fe(L)Cl_2](PF_6)$ behave as 1:1 electrolytes (120−160 Ω^{-1} cm^2 mol^{-1}). In contrast, in aqueous solutions the chloride anions are subject to dissociation to form the corresponding aquo/hydroxo complexes. The resulting aquo complexes can deprotonate to form hydroxo complexes, and those derivatives should have very different physical properties, e.g., redox potentials. Consequently, it is very important to know the proton dissociation constants of the coordinated water molecules. The deprotonation constants determine the distribution of different species at each pH and, consequently, establish the coordination environment around the metal center, i.e., ligands present and the coordination number. In Figure 2 the titration curve for a 2.31 mM aqueous $[Fe(L^1)Cl_2](PF_6)$ solution with 1.010 M NaOH is presented. In Table 1 the pK_a's for the Fe^{III} complexes in aqueous solutions obtained from the titration studies are presented. Each of the complexes exhibits two pK_a values, which indicates that two water molecules coordinate to the metal center in the Fe(III) complexes. Therefore, the complexes are seven-coordinate in aqueous solutions, assuming that all five nitrogens on the pentaaza macrocyclic ligand coordinate with iron. This implies that the chloride anions are replaced by water molecules. The pK_a values are quite similar for all of the complexes, falling in the ranges 3.5−4.1 and 7.3−

(16) Evans, D. F. *J. Chem. Soc.* **1959**, 2003.

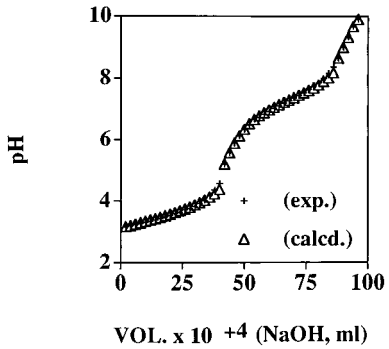

Figure 2. Experimental and calculated titration curves for 2.00 mL of 2.31 mM $[Fe(L^1)Cl_2](PF_6)$.

7.7 for the first and second proton dissociations, respectively (Table 1). These results suggest that the complexes are stronger acids than acetic acid. The pK_a's for the complexes with L^2 and L^3 are slightly higher than those for $[Fe(L^1)Cl_2](PF_6)$ and $[Fe(L^4)Cl_2](PF_6)$, and this is reflected in the pH values found for aqueous solutions of the complexes at comparable concentrations. Consequently, under the reaction conditions of interest (i.e., at or near physiological pH, ~7.4), these $Fe^{III}(L)$ complexes exist as an equilibrium mixture of the $[Fe(L)(OH)_2]^+$ and the $[Fe(L)(OH_2)(OH)]^{2+}$ complexes.

Electrochemistry. The enzymatic reactions between SOD and the superoxide anion are redox reactions. The oxidized form of the enzyme SOD's, such as an $Fe^{III}-SOD$, oxidize the superoxide anion to molecular oxygen and the reduced form of SOD reduces superoxide (or its conjugate acid, $HO_2^{\bullet}$[17]) to peroxide. This implies that a requirement for SOD activity be that the redox potential for the metal complex should fall between the redox potentials for the reduction and oxidation of superoxide anion, i.e., $E_{O_2-/O_2} < E_{Fe^{II}/Fe^{III}} < E_{O_2^-/HO_2^{\bullet}-}$ (−0.3 to +0.9 V[17,18]). From the data presented in this study (vide infra), the iron couple involved in this catalytic process clearly falls within this range. In acetonitrile solution, each of the four Fe^{III} complexes exhibits only one reversible redox wave in the scan range from −1.5 to +1.5 V vs E_{Ag/Ag^+}, which can be assigned to the Fe^{II}/Fe^{III} couple. The cyclic voltammogram for $[Fe(L^1)Cl_2](PF_6)$ in an acetonitrile solution purged with nitrogen exhibits a reversible couple at −0.19 V vs E_{Ag/Ag^+}, or −0.17 V vs NHE, obtained by calibration with ferrocene. The cyclic voltammogram for the complex $[Fe(L^1)Cl_2](PF_6)$ in an acetonitrile solution that has been saturated with air is strikingly different. When the scan starts at 0 V and proceeds toward negative potentials, the complex is reduced to an Fe^{II} species and exhibits a cathodic peak at −0.23 V. As the scan continues, molecular oxygen is reduced to superoxide at −1.15 V. When the scan is then returned to 0 from −1.4 V, no corresponding anodic peaks are found, in contrast to the reversible redox behaviors for both the Fe^{III} complex and dioxygen in acetonitrile solutions. The disappearance of the oxidation peak for the Fe^{II} species can be rationalized. The concentration of the Fe^{III} complex (0.8 mM) is less than that of oxygen; thus, the Fe^{II} species is present at lower concentration than superoxide ion, as was observed from the reduction currents in the cyclic voltammogram. Even without considering the possible oxidation of the Fe^{II} species by dissolved oxygen, it is impossible for Fe^{II} to consume all of the superoxide through a 1:1 chemical reaction. Hence, the disappearance of the oxidation peak for superoxide suggests that the iron complex catalyzes the decomposition of superoxide. In acetonitrile solution, the redox potentials for the other three complexes are quite similar to that for $[Fe(L^1)Cl_2](PF_6)$ (Table 2).

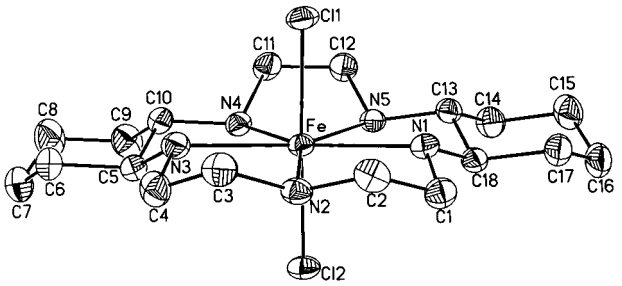

Figure 3. Projection view of the molecule $[Fe(L_2)Cl_2](PF_6)$ with non-hydrogen atoms represented by 50% probability ellipsoids.

In unbuffered aqueous solutions (pH ~ 3), three of the complexes, $[Fe(L^1)Cl_2](PF_6)$, $[Fe(L^2)Cl_2](PF_6)$, and $[Fe(L^3)Cl_2](PF_6)$, display well-defined redox couples in the scan range from −0.75 to +0.50 V vs SCE. The redox potential for $[Fe(L^1)Cl_2](PF_6)$ is 0.11 V vs SCE or 0.35 V vs NHE with a peak separation of 75 mV. The potential shifts 0.52 V toward more positive potentials, compared to the values observed in acetonitrile solution. Although a potential shift has been observed for other Fe^{II} complexes with pentadentate ligands derived from triazacycloalkanes,[19] such a large shift is unexpected. This large potential shift is attributed to the replacement of the two anions from the coordination sphere by two neutral water ligands. The Fe^{II}/Fe^{III} redox potentials for $[Fe(L^2)Cl_2](PF_6)$ and $[Fe(L^3)Cl_2](PF_6)$ are 100 mV higher than that for $[Fe(L^1)Cl_2](PF_6)$, again contrasting with the similarity of the redox potentials for the complexes in acetonitrile solutions. At pH = 2.6, $[Fe(L^1)Cl_2](PF_6)$ only shows one reduction peak; the disappearance of the anodic peak may be due to the dissociation of the Fe^{II} complex at low pH. In contrast, $[Fe(L^2)Cl_2](PF_6)$ exhibits reversible redox behavior even at pH = 2.09, but the anodic peak almost disappears at pH = 1.60. This implies that the more highly preorganized and rigid macrocycle containing the two *trans*-cyclohexano groups on the ligand stablizes the resultant Fe^{II} complex. In the scan range from −0.50 to +0.50 V vs SCE, $[Fe(L^4)Cl_2](PF_6)$ has one oxidation peak at 0.44 V vs NHE and two reduction peaks at 0.31 and 0.14 V vs NHE, respectively.

Crystal Structure of $[Fe(L^2)Cl_2](PF_6)$. The hexafluorophosphate salt of the Fe^{III} complex of L^2, $[Fe(L^2)Cl_2](PF_6)$, crystallizes in the triclinic space group $P\bar{1}$ (see Table 3 for pertinent crystal data). A projection view of the molecule with non-hydrogen atoms represented by 50% probability ellipsoids is presented in Figure 3, and selected bond lengths (Table 4), bond angles (Table 5), and atom coordinates (Table 6) are listed. The Fe^{III} is seven-coordinate with five nitrogen atoms from the macrocyclic ligand and two *trans*-chloro anions. The five N atoms are almost planar; thus, the coordination sphere can be best described as a pentagonal bipyramid. There are five chelate rings formed by Fe and N−C−C−N units. In these chelate rings, the N−C−C−N torsion prefers the gauche conformation, as observed in metal complexes with ethylenediamine and with the same family of ligands with Mn(II) complexes.[7,8] Four N−C−C−N torsion angles in this complex have a gauche conformation, while the fifth torsion N(4)−C(11)-C(12)−N(5) has a almost eclipsed conformation. For five planar N atoms, it is difficult for all five N−C−C−N torsion angles to have ideal gauche conformation (around 60°) at the same time. Two

(17) Sawyer, D. T.; Valentine, J. S. *Acc. Chem. Res.* **1981**, *14*, 393.
(18) Sawyer, D. T.; Tsang, P. K. S. *Free Radical Res. Commun.* **1991**, *12*−*13*, 75.
(19) Zhang. D. Ph.D. Dissertation, University of Kansas, 1994.

rigid cyclohexyl groups further force the N−C−C−N torsion connecting them to adopt an eclipsed conformation. This forces the molecule to adopt a pseudomirror symmetry, which passes through Fe, N(2), two chloro atoms, and the centroid of the bond C(11)−C(12). The eclipsed conformation increases strain in the N(4)−C(11)−C(12)−N(5) unit and results in the relatively larger N−C−C angle (111.1°), compared to the average angle of 107.1° in the other two diazaethane units.

The five Fe−N bond lengths are 2.290(3), 2.250(3), 2.280(3), 2.259(3), and 2.275(2) Å, with an average of 2.271 Å. The N atom not connected to the cyclohexyl groups possesses a shorter coordination bond, possibly due to its relative freedom. The five chelate angles N−Fe−N are 73.37(9), 73.72(10), 72.67(9), 69.11(9), and 72.39(0)°, with an average of 72.25°. The sum of the chelate angles is 361.2°, very close to 360° for an ideal planar structure. It is interesting to compare this structure with that of the corresponding $[Mn^{II}(L^2)Cl_2]$ complex containing the high-spin d^5 Mn^{II} ion in the identical ligand environment: the Mn^{II}−N bond distances are slightly longer, with the average distance at 2.31 Å, and the Mn−Cl distances are 2.56 and 2.63 Å,[20] whereas the Fe^{III} analogue with L^2 has Fe−Cl bond lengths of 2.33 and 2.35 Å. The shorter bond lengths undoubtedly are due to the smaller size/greater charge of the +3 high-spin d^5 Fe^{III} center.

Kinetics of Superoxide Decay and Mechanism Studies. Spontaneous superoxide decomposition in aqueous solution is a second-order reaction.[13] In the presence of superoxide dismutase, the decomposition of superoxide is much faster (at pH > 7) and the catalyzed reaction is first-order in superoxide concentration. For example, the reported rate for bacterial Fe−SOD is on the order of $3 \times 10^{+8}$ M^{-1} s^{-1}.[21] Examples of synthetic low molecular weight superoxide dismutase catalysts employing iron as the redox-active metal are relatively sparse. Only a few synthetic complexes have been reported, and these have been shown to possess modest catalytic SOD activity. For example, Fe^{III}(EDTA) has been reported to catalyze the dismutation at a rate approximately 10^3 times slower than the native enzymes.[22] Synthetic porphyrins containing iron also have been reported but suffer from catalytic deactivation owing to dimer formation.[23] We have previously reported that the Fe(III) complex of tris[*N*-(2-pyridylmethyl)-2-aminoethyl]amine (Fe-TPAA) was the most active Fe-based mimic which we had studied with a k_{cat} of $2.16 \times 10^{+6}$ M^{-1} s^{-1}.[23,24]

We have found that the Mn(II) complexes with pentaazacycloalkane ligands display very high SOD activity and catalyze the first-order decomposition of superoxide with rate constants as high as 1.2×10^8 M^{-1} s^{-1} at pH = 7.4.[7,8] For this reason we synthesized the corresponding Fe(III) complexes with some of our representative pentaazacycloalkane ligands in order to determine whether active synthetic Fe-based mimics could be synthesized.

The new Fe(III) complexes reported here are the first iron complexes to be synthesized with pentaazacycloalkanes and to be investigated as potential SOD mimics. Their redox potentials lie in a range such that both oxidized and reduced species can react with the superoxide, suggesting that catalytic SOD activity may be possible. The SOD activity assay/experiment is designed so that the initial concentration of superoxide ≫ [Fe^{III}(L)]. Under these conditions, the two general reactions governing the overall catalytic redox reaction are reduction of Fe^{III} (eq 1) and oxidation of a reduced Fe^{II} species with the strong

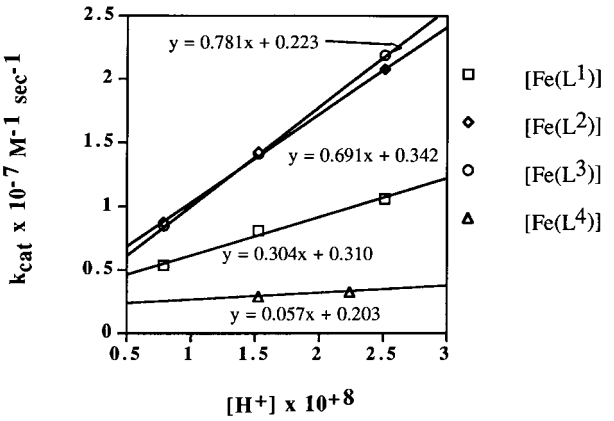

Figure 4. Dependence of pH on the k_{cat} for the new Fe^{III} complexes.

$$O_2^- + [Fe^{III}(L)] \xrightarrow{k_1} O_2 + [Fe^{II}(L)] \quad (1)$$

$$HO_2^\bullet + [Fe^{II}(L)] \xrightarrow{k_2} HO_2^- + [Fe^{III}(L)] \quad (2)$$

oxidant $HO_2^\bullet$.[20] Since the initial concentration of O_2^- is much larger than the catalyst concentration, the amount of O_2^- consumed by the Fe^{III} species must equal that reacting with Fe^{II}, assuming no reaction between the iron complexes and other compounds, such as hydrogen peroxide. From eq 3, it can been

$$d[O_2^-]/dt = \{k_1[Fe^{III}(L)] + k_2([Fe^{II}(L)][H^+]/K_a])\}[O_2^-] \quad (3)$$

$$K_a = [O_2^-][H^+]/[HO_2]$$

$$k_{obs} = k_1[Fe^{III}(L)] + k_2'[Fe^{II}(L)] = (k_1\alpha_{Fe^{III}(L)} + k_2'\alpha_{Fe^{II}(L)})[Fe]_{tot} \quad (4)$$

$$k_2' = k_2[H^+]/K_a$$

$$k_{cat} = k_{obs}/[Fe]_{tot} = (k_1\alpha_{Fe^{III}(L)} + k_2'\alpha_{Fe^{II}(L)}) \quad (5)$$

$$k_{cat} = 2k_1\alpha_{Fe^{III}(L)} = 2k_2\alpha_{Fe^{II}(L)} \quad (6)$$

seen that the decomposition of superoxide catalyzed by metal complexes is first-order in superoxide. The first-order rate constant contains the constant concentration of the catalyst.

The k_{obs} values measured for these four new Fe^{III} complexes under conditions of varying pH all show pure first-order superoxide decay behavior. The k_{cat} for a particular Fe^{III} complex is obtained from the plot of the k_{obs} value versus the initial concentration of Fe^{III} complex. The slopes of these plots are equal to the k_{cat} value at a given pH.[13] In Figure 4 are shown the values for k_{cat} for the four new complexes over a range of pH. For three of the four complexes, the k_{cat} increases linearly as the pH decreases. In contrast, the complex Fe(L^4) is insensitive to the pH. This pH-dependent phenomenon has also been observed for the manganese(II) complexes with the same three pentaazacycloalkane ligands, and pH independence was also observed with the analogous Mn^{II} complex of ligand L^4. For the Mn^{II}(L) complexes, this behavior has been rationalized

(20) Riley, D. P.; Lennon, P. J.; Neumann, W. L.; Weiss, R. H. *J. Am. Chem. Soc.* **1997**, *119*, 6522.
(21) (a) Fee, J. A.; McClune, G. J.; O'Neill, P.; Fielden, E. M. *Biochem. Biophys. Res. Commun.* **1981**, *100*, 377. (b) Lavelle, F.; McAdam, M. E.; Fielden, E. M.; Puget, K.; Michelson, A. M. *Biochem. J.* **1977**, *161*, 3.
(22) McClune, G. J.; Fee, J. A.; McClusky, G. A.; Groves, J. T. *J. Am. Chem. Soc.* **1977**, *99*, 5220.
(23) Weiss, R. H.; Flickinger, A. G.; Rivers, W. J.; Hardy, M. M.; Aston, K. W.; Ryan, U. S. *J. Biol. Chem.* **1993**, *268*, 23049.
(24) Nagano, T.; Hirano, T.; Hirobe, M. *J. Biol. Chem.* **1989**, *264*, 9243.

in terms of a mechanism that is a combination of two separate rate-determining steps: a pH-dependent and a pH-independent process. The pH-dependent process is not operative with the pentamethyl ligand L[48], but with the remaining complexes, it can play a dominant role in the rate at physiological pH. This pH-dependent process involves reduction of protonated superoxide $HO_2^{\bullet}$ via proton-coupled electron transfer from Mn(II), i.e., H atom transfer from a bound water to $HO_2^{\bullet}$.[20] Proton-coupled electron transfer is gaining experimental support as an important pathway of electron transfer in biological systems such as photosystem II,[25] as this path does not require charge separation to build up in the transition state. Recent thermodynamic data show that the bond dissociation energy (BDE) of an O−H bond of a water bound to a Mn^{III}(Salen) derivative is 86 kcal/mol.[26] Thus, H atom transfer to $HO_2^{\bullet}$ is energetically allowed as the BDE of the O−H bond of hydrogen peroxide is reported to be 87.2 kcal/mol.[27]

In contrast, the pH-independent step involves prior binding of superoxide anion to a vacant coordination site on Mn(II) followed by fast oxidation of the Mn^{II} complex—a process dependent on the rate of generation of vacant coordination sites on the Mn(II) center. However, for the Fe^{III} complexes, the deprotonation of coordinated water molecules must be taken into account, since the aquo Fe(III) complexes described are much stronger acids than the corresponding aquo Mn(II) complexes, for which the first pK_a of the axial bound water is ∼11.2.[8] Thus, the axial-site ligand speciation is much more critical for these Fe(III) complexes. At the pH range in which the k_{cat} determinations are made (pH ∼ 7.6−8.1) most of the Fe^{III}(L) complex is in the dihydroxo form, $[Fe(L)(OH)_2]^+$.

To probe the mechanism of this system further, we utilized the complex with L^2 for further spectrophotometric studies. The intense (ϵ ∼9400) and isolated absorption band (λ_{max} = 294 nm) of this complex made it possible to probe the nature of the rate-determining step in this catalytic system. Using $[Fe(L^2)Cl_2]^+$ in water with HEPES buffer at pH = 7.55, we studied the decay of superoxide under catalytic conditions ($[O_2^{\bullet-}]/[Fe] > 8$) in which the spectral region from 230 to 420 nm is monitored using an OLIS rapid-scan spectrophotometer stopped-flow system. In this way, both the superoxide decay (λ_{max} = 245 nm, ϵ ∼2200) and any change in the spectrum of the Fe^{III} complex can be monitored simultaneously at 294 nm. In this series of experiments at pH = 7.55, the Fe^{III} complex is present as an approximately 1:1 mixture of the $[Fe(L)(OH)_2]^+$ and $[Fe(L)(OH)OH_2)]^{2+}$ complexes. During the entire course of the first-order decay of the superoxide (complete in 40 ms), no change is observed in the spectrum of the Fe^{III} complex. This result clearly indicates that reduction of high-spin d^5 Fe^{III} to Fe^{II} is rate-determining during this catalytic process and that throughout the reaction most of the Fe is present as Fe^{III}. This is the inverse of the situation for the Mn^{II} system, in which oxidation of the corresponding high-spin d^5 metal ion is rate-determining.

If reduction of an Fe^{III} complex to an Fe^{II} complex is rate-determining, it is logical, on the basis of electrochemical data, that since the $[Fe^{III}(L)(OH)(OH_2)]^{2+}$ complex is far easier to reduce than the dihydroxo Fe^{III}(L) complex, it is indeed the catalytically active species in this system. This also means that the reduction of an aquo hydroxo Fe^{III}(L) complex occurs by an inner-sphere binding to Fe^{III}. This requires the loss of a bound axially coordinated water molecule. The rates of the water exchange on the Fe^{III} complex may then be rate-limiting, and the generation of the vacant coordination site governs the catalytic rate. In general, water exchange rates on high-spin Fe^{III} in acid are measured to be faster than 10^{+3} s^{-1} and several orders of magnitude faster than this when the pH is higher and a hydroxo ligand is bound to Fe^{III}, labilizing the *trans*-aquoligand to dissociation.[28] The rate of catalysis observed with these complexes requires that k_{off} for the bound water be on the order of 10^{+7} s^{-1}, a value entirely consistent with a water bound to the high-spin Fe^{III} center with a *trans*-hydroxo—as occurs with this system.

To probe this further, the catalytic rate of superoxide disproportionation was studied in D_2O at pH = 7.55.[29] In D_2O, the rate of water exchange with the bound Fe^{III} may show a slight secondary isotope effect, since the isotope effect observed in H_2O (D_2O) for water exchange on +3 metal ions is expected to be small, as is observed with +3 lanthanide ions.[30] In contrast, a large inverse isotope effect should be expected (perhaps as large as 3). This unusual effect would be predicted because the pK_a of a coordinated heavy water will be higher than that of a bound light water; thus, the equilibrium concentration of the $[Fe^{III}(L)(OH)(OH_2)]^{2+}$ complex will be shifted, so that at any pH in the range 7.4−8.1 the D_2O system will contain a higher concentration of active catalytic species, $[Fe^{III}(L)(OH)(OH_2)]^{2+}$. Thus, a faster apparent rate should be observed in D_2O because there will be a higher concentration of the active form of the catalyst. At pH = 7.60 the rate of dismutation of superoxide was measured with the complex $[Fe^{III}(L^2)Cl_2]^+$, and in D_2O the k_{cat} was found to be $4.41 \times 10^{+7}$ M^{-1} s^{-1}—corresponding to a rate enhancement of 2.13 times that observed in light water. This result provides additional support for the conclusion that generation of a vacant coordination site on the Fe^{III} followed by rapid binding to Fe^{III} by superoxide with subsequent reduction of Fe^{III} (eqs 7−9) is

$$[Fe^{III}(L)(OH)(OH_2)]^{2+} \rightarrow [Fe^{III}(L)(OH)]^{2+} + H_2O \quad (7)$$

$$[Fe^{III}(L)(OH)]^{2+} + O_2^{\bullet-} \rightarrow [Fe^{III}(L)(OH)(O_2)]^{+} \quad (8)$$

$$[Fe^{III}(L)(OH)(O_2)]^{+} \rightarrow [Fe^{II}(L)(OH)]^{+} + O_2 \quad (9)$$

operating in this catalytic system. Thus, if $[Fe(L)]_{tot} \sim [Fe^{III}(L)]$, then k_{obs} is approximated by the expression of eq 10. Since

$$k_{obs} = k_1[Fe^{III}(L)(OH)(OH_2)]^{2+} \quad (10)$$

the concentration of the aquo hydroxo species is related to the total $[Fe^{III}]$ by the K_a' of the second bound water, the k_{obs} becomes as defined in eq 11. $[Fe]_{total}([H^+]/([H^+] + K_a'))$ is equal

$$k_{obs} = k_1[Fe^{III}(L)]_{tot}([H^+]/([H^+] + K_a')) \quad (11)$$

to the concentration of aquo hydroxo species. From these equations, k_{cat} is pH dependent, and the plot of $[H^+]/([H^+] + K_a)$ versus $[H^+]$ would generate a curve over a wide enough pH range. However, if $[H^+] \ll K_a$, k_{cat} is equal to $2k_1[H^+]/(K_a)$, which has a linear relationship with $[H^+]$. On the other

(25) Haganson, C. W.; Lydakis-Simantris, N.; Tang, X.; Tommos, C.; Warncke, K.; Babcock, G. T.; Diner, B. A.; McCracken, J.; Styring, S. *Photosynth. Res.* **1995**, *46*, 177.
(26) Caudle, M. T.; Pecoraro, V. L. *J. Am. Chem. Soc.* **1997**, *119*, 3415.
(27) Howard, C. J. *J. Am. Chem. Soc.* **1980**, *102*, 6937.
(28) Basolo, F.; Pearson, R. G. *Mechanisms of Inorganic Reactions;* John Wiley & Sons: New York, 1967; Chapter 3, pp 145−158.
(29) Covington, A. K.; Paabo, M.; Robinson, R. A.; Bates, R. G. *Anal. Chem.* **1968**, *40*, 501.
(30) Reidler, J.; Silber, H. B. *J. Phys. Chem.* **1973**, *77*, 1275.

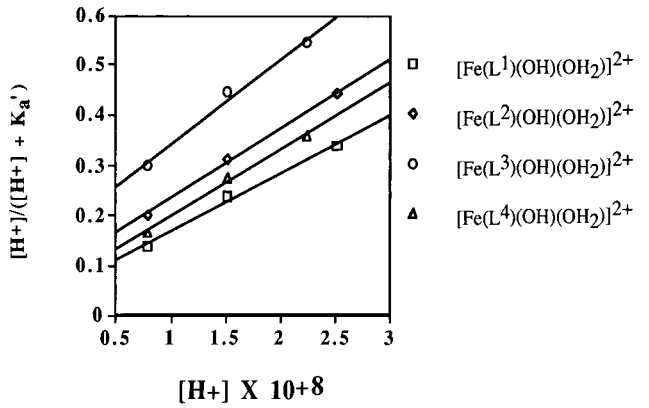

Figure 5. Relationship between the concentration of the $[Fe(L)(OH)(OH_2)]^{2+}$ species and the pH of the solution.

hand, when $[H^+] \gg K_a$, k_{cat} is equal to $2k_1$ and is pH independent. In this system near physiological pH (7.4), $[H^+]$ is approximately the value of K_a' for these four Fe^{III} complexes. As discussed earlier, the Fe^{III} complexes are seven-coordinate with five nitrogen atoms from the macrocyclic ligand and two oxygens from water molecules or hydroxide ions. The pK_a's for the water molecules indicate that $[Fe^{III}L(H_2O)(OH)]^{2+}$ and $[Fe^{III}L(OH)_2]^+$ are dominant species in solution under the conditions of interest near physiological pH. Assuming that reduction (eq 1) is the rate-determining step and $[Fe^{III}(L)(H_2O)(OH)]^{2+}$ is the active species, the plots of the fraction of the aquo hydroxo species ($[H^+]/([H^+] + K_a')$ against $[H^+]$ are presented in Figure 5 for the four Fe^{III} complexes using their experimentally derived K_a' values (Table 1). It can be seen from the data over this pH range that the $[H^+]$ dependence on the k_{cat} rate for these complexes is indeed expected to be linear on the basis of the dependence of the rate on the concentration of the active catalytic species, $[Fe^{III}(L)(H_2O)(OH)]^{2+}$.

Three of these complexes (with L^1, L^2, L^3) are in excellent agreement with this rationale for pH dependence. The complex with the pentamethyl ligand ($[Fe(L^4)Cl_2]^+$) clearly does not appear to fit with this explanation of pH dependence, since this complex has virtually no pH dependence on its catalytic rate. It is not clear why this complex possesses a lower catalytic activity with a pH behavior unlike the other complexes, as its redox potential and bound water pK_a values are virtually identical. Possible explanations are (1) that this complex readily undergoes ligand modification under conditions of catalysis (presence of an excess of strong oxidant + strong reductant) producing an altered catalyst (e.g., imine formation) with different bound water pK_a values and a slower inherent rate for superoxide dismutation and (2) that the complex may more readily form oxo-bridged dimers with lower inherent k_{cat} values than a monomeric structure and pK_a values not in the range of the pH of interest for these studies. The latter explanation is not consistent with the observed first-order rate dependence of k_{cat} on the concentration of $[Fe(L^4)Cl_2]^+$, but the presence of other species arising from ligand oxidation processes is consistent with the observation of two additional reduction processes observed in the cyclic voltammetry for this complex. None of the other complexes exhibit the new waves. Thus, it is likely that the behavior observed with the complex derived from L^4 may arise from redox chemistry occurring on the ligand itself.

From our studies, we find that the pH of the solution influences k_{cat} by changing the distribution of the different solvated Fe^{III} complexes. If other factors are similar, a higher pK_a for the aquo ligand will raise the k_{cat}—as is observed here. This mechanistic insight should aid in the design of ligands which will promote enhanced SOD activity by decreasing the acidity of the second bound water on the Fe^{III} center. In conclusion, we are continuing to pursue the goal of enhanced catalytic activity for these Fe^{III}-based SOD catalysts by modifying the pentaaza macrocyclic ligand structure with substituent variations which allow us to alter the bound water pK_a while retaining ligands which are not subject to oxidative change themselves.

Acknowledgment. The authors thank Mr. Karl Aston, Mr. Hayat Rahman, Mr. Willie Rivers, and Mr. Kirby Sample for their outstanding technical assistance.

Supporting Information Available: Tables listing the positional and isotopic displacement coefficients for hydrogen atoms and the anisotropic displacement coefficients for the non-hydrogen atoms (2 pages). See any current masthead page for ordering information.

IC970861H